A CRITERION FOR PREDICTING DUCTILE-BRITTLE TRANSITION BEHAVIOUR IN HY100 STEEL UNDER MIXED MODE I/II LOADING

D. Bhattacharjee* and J.F. Knott†

In quenched and tempered HY100 steel, crack initiation is tensile stress controlled at low temperatures (e.g., at -196 °C), and is shear displacement (or strain) controlled at higher temperatures (e.g., room temperature). The temperature at which the transition in the micromechanism of fracture occurs is found to be dependent on the mixed mode ratio such that with increasing Mode II component, the transition temperature decreases. Based on crack tip shear displacement, a model is proposed in this paper which is able to predict the fracture behaviour (and hence the ductile-brittle transition) given the temperature and the load.

INTRODUCTION

Subjecting a crack tip to different ratios of Mode I and Mode II loading predictably changes the direction of the maximum tensile stress. Testing under mixed mode loading serves two purposes. First, it provides a way of predictably varying the stress field ahead of the crack tip; secondly, it emulates the practical situation where cracks in a structure are oriented at angles other than 90° to the remote load. This paper reports the studies made on the effect of mixed mode loading on the micromechanism of crack initiation and its consequent effect on the ductile-brittle transition temperature.

It is observed that at liquid nitrogen temperature (-196 °C) the crack propagates in a direction normal to the maximum tensile stress ahead the crack tip for a wide range of Mode I/II ratios. Since the maximum tangential stress acts at angles other than 90° to the starter crack plane in the mixed mode case, crack propagation occurs at an angle to the starter crack. These angles are predicted by the various LEFM based fracture criteria e.g., Erdogan and Sih (1), Sih (2) and Hussain et al (3).

*Department of Materials Science and Metallurgy, University of Cambridge, Pembroke Street, Cambridge CB2 3QZ, U.K.
†School of Metallurgy and Materials, University of Birmingham, Edgbaston, Birmingham, B15 2TT, U.K.

With increasing temperature, a transition in the micromechanism of fracture occurs whereby crack initiation and growth cease to be tensile stress controlled and become shear displacement (or shear strain) controlled, as shown by Bhattacharjee and Knott (4). The temperature at which the micro-mechanism of fracture changes, is defined as the transition temperature, T_{tr} (the ductile-brittle transition temperature). Above this transition temperature, fracture initiates in a localised slip band, at a critical value of the crack tip shear displacement, irrespective of the Mode I/II ratio (except for the pure Mode I case) (4). The macroscopic difference in fracture behaviour above and below the transition temperature is shown in Fig. 1 which shows two specimens which were subjected to similar mixed mode ratios, but were tested at different temperatures. The specimen shown at the bottom was tested below T_{tr} and crack propagation occurs at an angle to the starter crack; the specimen shown at the top was tested above T_{tr} where crack initiation and propagation occur along a shear band, coplanar with the starter crack (Bhattacharjee and Knott (5)).

A notch with a small semi-circular root radius, under a combination of tension and shear loading, has been shown, both experimentally (4) and theoretically (Aoki et al (6)), to deform in a manner such that one side of it blunts while the other side sharpens. The maximum tensile stress is located on the blunted side while the shear strain is located on the sharpened side. It is thus suggested that a competition exists between a tensile stress controlled failure at the blunted side and a shear strain controlled failure at the sharpened side. The final failure mechanism depends upon the result of this competition which depends upon the microstructural properties (carbide distribution, work hardening capacity, etc.) and yield stress, which is a function of temperature and determines the magnitudes of tensile stress on the blunted side and shear strain on the sharpened side.

In this paper a model is developed, based on the crack tip shear displacement, which would predict the fracture behaviour (i.e., whether tensile stress controlled or shear strain controlled), given the temperature and the load.

EXPERIMENTAL

The chemical composition of the material used and the heat treatment schedule have been discussed in references (4) and (5). The test pieces possessed a tempered martensite microstructure with fine cementite particles distributed in a ferrite matrix. The variation of yield strength (0.2% proof stress) of the material with temperature is shown in Fig. 2.

The nominal dimensions of the edge-cracked test-pieces tested at -196 °C were: length L = 100mm, breadth B = 8mm, width W = 16mm and a/W = 0.5, where a is the crack length. In order to accommodate the increasing plastic zone size with increasing temperature, the nominal dimensions of the specimens tested above -196 °C were increased to B = 10mm and W = 20mm. L remained at 100mm and the a/W ratio of 0.5 was maintained. Mixed mode loading was achieved by using an asymmetric four-point bend configuration, the details of which are given in reference (5). The Mode I and Mode II stress intensity factors (K_I and K_{II}, respectively) have been given by Suresh et al (7) as:

$$K_I = \frac{PS_o}{3BW^2}\sqrt{\pi a}\,Y_I \quad \text{and} \quad K_{II} = \frac{P}{3BW}\sqrt{\pi a}\,Y_{II} \tag{1}$$

In Eqn. (1), P is the load, S_o is the distance of the starter crack from the centre line of the configuration (which controls the mixed mode ratio) and Y_I and Y_{II} are dimensional calibration functions which depend upon the a/W ratio.

The starter cracks were introduced as slits of 0.16mm width using SiC slitting wheels. Some specimens were pre-fatigued to obtain an a/W ratio of 0.5. Under identical conditions of testing temperature and mixed mode ratio, the fracture behaviour of the as-slit and pre-fatigued specimens was found to be similar both in the nature of the fracture surface and the load-displacement trace.

The tests at low temperatures were carried out in a bath which could hold a cooling liquid around the loading fixture and the test piece. Tests at -196 °C were carried out under liquid nitrogen. The other sub-zero temperatures were obtained by mixing methanol with liquid nitrogen in different ratios.

EFFECT OF MIXED MODE RATIO ON TRANSITION TEMPERATURE

Table 1 summarises the effect of mixed mode ratio on the fracture behaviour in the temperature range 20 °C to -140 °C. In the table, "shear" signifies crack growth through a shear band, as observed at room temperature, and "tensile" signifies a tensile stress controlled fracture behaviour, as seen at -196 °C. The thick line in Table 1 marks the transition temperature. Evidently, the transition temperature decreases as the Mode II component increases.

TABLE 1 – Summary of transition behaviour.

Temp	K_I/K_{II}						
(°C)	0.6	0.9	1.6	2.2	3.1	3.8	4.7
20	Shear	Shear	Shear	Shear	Shear	Shear	Shear
-50	Shear	Shear	Shear	Shear	Shear	Shear	Shear
-70			Shear	Shear	Shear	Tensile	Tensile
-80			Shear	Tensile	Tensile	Tensile	Tensile
-90		Shear	Shear	Tensile	Tensile	Tensile	
-100	Shear	Shear	Tensile	Tensile			
-110	Shear	Shear	Tensile				
-120	Shear	Tensile					

CRACK-TIP SHEAR DISPLACEMENT

Theory

It was shown in a previous paper (4) that above the transition temperature, crack initiation occurred at a constant value of crack tip shear displacement irrespective of

the mixed mode ratio. This critical crack tip shear displacement, d_p, was measured from the load versus shear displacement curve and was found to be about 0.4mm for quenched and tempered HY100 steel. Because of the way the shear displacement was measured, these values correspond to the *plastic* shear displacement at the crack tip. Any predictive model or criterion should be able to quantify the plastic shear displacement at the crack tip at any given load and temperature and compare this with the experimentally determined critical value for the same material. Thus, in order to obtain a predictive set of equations, the relationship between plastic shear displacement, load, mixed mode ratio and temperature has to be established.

In the pure Mode I case the crack tip opening displacement (COD) can be separated into its elastic component ($\delta_{I(el)}$) and the plastic component ($\delta_{I(pl)}$), such that

$$\delta_I = \delta_{I(el)} + \delta_{I(pl)} \tag{2}$$

It is possible to calculate the elastic component of COD for a given load from the relationship between $\delta_{I(el)}$ and the Mode I stress intensity factor (see e.g., Knott (8)). There is, however, no generally-accepted standard method available to calculate the plastic component directly from the applied load: $\delta_{I(pl)}$ is determined only experimentally.

Analogous to the case of the opening crack, it may be assumed that in the case of shear the crack shear displacement (CSD or δ_{II}) can also be separated into its elastic component, $\delta_{II(el)}$, and a plastic component, $\delta_{II(pl)}$. Thus,

$$\delta_{II} = \delta_{II(el)} + \delta_{II(pl)} \tag{3}$$

Bilby et al (9) expressed shear displacement at the crack tip as:

$$\delta_{II} = \frac{8\tau_y(1-\nu^2)a}{\pi E} \ln\left[\sec\left(\frac{\pi\tau}{2\tau_y}\right)\right] \tag{4}$$

where ν is the Poisson's ratio and E is the Young's modulus. If only low values of τ/τ_y are considered in the expansion of the lnsec term (i.e., considering only the first term in the expansion and thus limiting behaviour to the quasi-elastic regime), Eqn. (4) may be simplified to:

$$\delta_{II(el)} = \frac{\sqrt{3}\, K_{II}^2\,(1-\nu^2)}{\sigma_y E} \tag{5}$$

where $\tau_y = \sigma_y/\sqrt{3}$ if von Mises yield criterion is followed.

Ideally, a critical shear displacement criterion suggests that the plastic shear displacement component, $\delta_{II(pl)}$, must reach the critical value (d_p) for a shear crack to initiate. However, we are not in a position to determine $\delta_{II(pl)}$ from a given load. Therefore, the approach taken here is to associate a critical elastic displacement to the plastic component of the displacement. The justification for such an approach is that

both $\delta_{II(el)}$ and $\delta_{II(pl)}$ are related to the applied load, and both increase with increasing load. Had the relationship of $\delta_{II(pl)}$ with applied load been known, then by eliminating the load term from that equation and Eqn. (5) it would have been possible to establish a relationship between $\delta_{II(el)}$ and $\delta_{II(pl)}$.

It is suggested here that when $\delta_{II(pl)}$ reaches the critical value d_p, the corresponding elastic component also indicates a critical limit. This approach makes it possible for $\delta_{II(el)}$ to be calculated from Eqn. (5) for any given load and compare the calculated values with the *critical* $\delta_{II(el)}$ value corresponding to the *critical* plastic displacement. The term $\delta_{II(el)}$ is a function of the shear stress, τ, or K_{II} (Eqn. (5)), so that, although d_p is independent of mixed mode ratio, the critical value of $\delta_{II(el)}$ depends upon the Mode I/Mode II ratio.

Critical elastic component of shear displacement ($\delta^{crit}_{II(el)}$). Table 2 lists the d_p values for the test pieces for which d_p was experimentally measured. P_i corresponds to the load at crack initiation. The experimental techniques used for measuring d_p and P_i are described in reference (4). K_{II} was calculated using P_i in Eqn. (1). Since the measurements of d_p were made at room temperature, the value of yield stress used is 1050 MPa.

The $\delta^{crit}_{II(el)}$ values corresponding to the experimentally obtained d_p values are plotted in Fig. 3. A best fit straight line is drawn, connecting the $\delta^{crit}_{II(el)}$ values. This line marks the *critical elastic* shear displacement which must be reached so that the plastic component attains its critical value. In order to take experimental scatter into account, two dashed lines are drawn in Fig. 3 which enclose the experimental points. Thus the region between the dashed lines marks the transition regime. If the calculated value of $\delta_{II(el)}$ lies within $\delta^{crit}_{II(el)} \pm 0.003$mm, or is above the transition regime, then fracture is predicted to be shear strain controlled.

The best fit line in Fig. 3 follows the following relationship:

$$\delta^{crit}_{II(el)} = 0.054738 - 0.00039574 \ (\arctan \ (K_I/K_{II})) \qquad (6)$$

The dependence of $\delta^{crit}_{II(el)}$ on the mixed mode ratio is clear. However, it is necessary to investigate the effect of temperature on $\delta^{crit}_{II(el)}$.

TABLE 2 – Values of *critical* elastic shear displacement.

K_I/K_{II}	P_i (kN)	K_{II} (MPa$\sqrt{m}$)	d_p (mm)	σ_y (MPa)	$\delta^{crit}_{II(el)}$ (mm)
2.20	150.5	59.07	0.401	1050	0.027
1.57	167.0	67.40	0.387	1050	0.032
1.57	172.5	69.60	0.401	1050	0.034
0.94	181.5	72.35	0.370	1050	0.038
0.94	176.0	70.96	0.369	1050	0.034
0.63	187.5	73.94	0.401	1050	0.042

Effect of temperature on critical shear displacement

Here it is also assumed that d_p remains constant irrespective of temperature. This assumption may be justified by the micromechanism of plastic damage proposed in reference (4) in which d_p is associated with a critical number of dislocations in a pile-up at carbide/matrix interface. The critical shear strain obtained from d_p was very close to the value predicted by the dislocation model. The microstructural parameters (carbide particle size, interface strength, etc.) and bulk parameters (elastic constants) that were used to calculate the theoretical shear strain are not strong functions of temperature. It is therefore thought reasonable to assume d_p to be independent of temperature.

With decreasing temperature the yield stress has been shown to increase (Fig. 2). This implies that for a given load, the plastic displacement decreases with decreasing temperature. It is clear from Eqn. (5) that the elastic component also decreases with increasing yield stress. However, the elastic and plastic components of displacement may not bear the same relationship with temperature. For a coarse grained martensitic microstructure Bowen [9] has shown that when σ_y = 1140MPa, typically $\delta^{crit}_{(el)} \approx \delta^{crit}_{(pl)}$, i.e., the elastic component contributes 50% of the total displacement. For the same microstructure, when σ_y = 600MPa, typically $\delta^{crit}_{(el)} \approx \delta^{crit}_{(pl)}/3$, i.e., the elastic component contributes only 25% of the total displacement. Therefore, with increasing yield stress the magnitude of the elastic component increases with respect to the magnitude of the plastic component. It is also observed that as the yield stress doubles, the contribution of the elastic component also doubles. Thus the lower the temperature, the higher will be the value of the elastic displacement component for which the plastic component attains the critical plastic displacement (d_p). Therefore, $\delta^{crit}_{II(el)}$ increases with decreasing temperature.

Following this argument, we assume that the critical value of the elastic displacement changes with temperature in the same manner as does the yield stress. In other words,

$$\Delta\delta^{crit}_{II(el)} \propto \Delta\sigma_y \tag{7}$$

where Δ stands for *(final - original)/original*. Therefore, the value of $\delta^{crit}_{II(el)}$ at any temperature T_1 ($|\delta^{crit}_{II(el)}|_{T_1}$) is given by:

$$|\delta^{crit}_{II(el)}|_{T_1} \approx \frac{|\sigma_y|_{T_1} - |\sigma_y|_{T_o}}{|\sigma_y|_{T_o}} |\delta^{crit}_{II(el)}|_{T_o} + |\delta^{crit}_{II(el)}|_{T_o} \tag{8}$$

where temperature $T_o > T_1$. Since room temperature was the highest temperature used in the experiments, T_o was taken to be 20 °C. Therefore, $|\sigma_y|_{T_o}$ = 1050MPa.

The values of $\delta^{crit}_{II(el)}$ for some mixed mode ratios and at different temperatures are listed in Table 3. The values of $|\delta^{crit}_{II(el)}|_{T_o}$ for the different mixed mode ratios (at 20 °C) have been obtained from Eqn. (6). The effect of temperature on the $\delta^{crit}_{II(el)}$ lines is shown in Fig. 4.

TABLE 3 – Effect of temperature on critical elastic displacement.

T (°C)	20			-100			-196		
σ_y (MPa)	1050			1200			1450		
K_I/K_{II}	0.63	1.66	3.15	0.63	1.66	3.15	0.63	1.66	3.15
$\lvert\delta^{crit}_{II(el)}\rvert_T$	0.042	0.032	0.026	0.048	0.036	0.030	0.058	0.044	0.036

VALIDATION OF THE MODEL

The theory developed in the previous section results in the straight lines in Fig. 4 which represent the limits defined by the values of $\delta^{crit}_{II(el)}$. For any specimen, the value of $\delta_{II(el)}$ must reach the value corresponding to the line in Fig. 4 in order for $\delta_{II(pl)}$ to attain the critical value of d_p. Therefore, for specimens which failed by crack propagation in shear (from the sharp side of the notch), the $\delta_{II(el)}$ value calculated from the load at initiation should be equal to or greater than the $\delta^{crit}_{II(el)}$ value predicted by the straight line corresponding to the test temperature. On the other hand, if failure occurs from the blunted side of the deforming notch (tensile stress controlled), then it is likely that the $\delta_{II(el)}$ value at fracture would be less than the value of $\delta^{crit}_{II(el)}$.

Table 4 lists the $\delta_{II(el)}$ values for specimens tested at three different temperatures and under different mixed mode ratios. For specimens which failed in tension, the load at failure, P_f, was used for the analysis, and for specimens which failed in shear, the load at initiation, P_i, was used. The comments in the "Prediction" column specify the failure mechanism as predicted by the comparison of $\delta_{II(el)}$ values with the value of $\delta^{crit}_{II(el)}$. "Shear" indicates shear failure, through a shear band, as exhibited above transition temperature and is predicted if $\delta_{II(el)} \geq \delta^{crit}_{II(el)}$, taking experimental error into account. "Tension" indicates failure below the transition temperature and is predicted if $\delta_{II(el)} < \delta^{crit}_{II(el)}$. The last column in Table 4 lists the observed crack propagation direction. Since no pure Mode I specimen is listed in this table, an angle of 0° indicates observed shear fracture. A non-zero fracture angle indicates that tensile stress controlled fracture behaviour is observed.

Since, in the mixed mode case, tensile stress controlled cracks propagate at an angle to the starter crack or notch and a crack growing through a shear band propagates nearly coplanar with the starter crack, it is evident from the above table that the predictions match very well with the observations.

CONCLUSIONS

1. The crack tip shear displacement has been separated into a plastic component and an elastic component. It is suggested that a shear crack initiates when the plastic component reaches a critical value. However, the relationship between this plastic component and the external load and temperature is not known. However, these variable relate directly to the *elastic* shear displacement component.

TABLE 4 – $\delta_{II(el)}$ values for specimens tested at various temperatures and under different mixed mode ratios.

Temp. (°C)	K_I/K_{II}	P_f (or P_i) (kN)	K_{II} MPa√m	σ_y (MPa)	$\delta_{II(el)}$ (mm)	$\delta^{crit}_{II(el)}$ (mm)	Pre-diction	Fracture angle (°)
-196	2.84	73.5	41.67	1450	0.010	0.037	Tensile	-31.5
	1.95	87.5	46.39	1450	0.012	0.042	Tensile	-35.0
	0.78	124.0	69.95	1450	0.027	0.055	Tensile	-58.0
	0.40	127.0	72.54	1450	0.029	0.064	Tensile	-60.5
-80	3.15	118.2	46.85	1155	0.015	0.028	Tensile	-44.0
	2.2	156.5	62.04	1155	0.026	0.032	Tensile	-52.5
	1.66	185.6	73.56	1155	0.037	0.034	Shear	0°
	0.63	216.5	85.83	1155	0.050	0.045	Shear	0°
20	3.15	137.5	54.39	1050	0.023	0.026	Shear	0°
	2.2	153.5	60.85	1050	0.028	0.029	Shear	0°
	1.66	178.8	70.88	1050	0.037	0.032	Shear	0°
	0.63	192.3	76.24	1050	0.044	0.042	Shear	0°

2. A critical *elastic* shear displacement, $\delta^{crit}_{II(el)}$, has been defined corresponding to the critical plastic component. $\delta^{crit}_{II(el)}$ is found to be dependent on both mixed mode ratio and temperature.

3. According to the model, if at any initiation load, $\delta_{II(el)} \geq \delta^{crit}_{II(el)}$, shear strain dominated fracture is predicted. Otherwise the fracture is predicted to be tensile stress controlled. Experimental results validate the predictions of the model.

ACKNOWLEDGEMENT

The authors are grateful to Professor C.J. Humphreys for providing the research facilities at the University of Cambridge.

SYMBOLS USED

δ_I, δ_{II} = Crack tip opening (COD) and shear (CSD) displacement respectively (mm).

$\delta_{I(el)}$, $\delta_{II(el)}$ = Elastic component of COD, CSD respectively (mm).

$\delta_{I(pl)}$,$\delta_{II(pl)}$ = Plastic component of COD, CSD respectively (mm).

$\delta^{crit}_{(el)}$, $\delta^{crit}_{(pl)}$ = Critical values of elastic and plastic displacements.

$\delta^{crit}_{II(el)}$ = Critical elastic crack tip shear displacement (mm).

d_p = Critical plastic crack tip shear displacement (mm).

K_I, K_{II} = Mode I and Mode II stress intensity factors (MPa$\sqrt{m}$).

ν = Poisson's ratio, taken to be 0.33.

E = Young's Modulus, taken to be 200 GPa.

REFERENCES

(1) Erdogan, F and Sih, G.C., Trans. ASME, J. Basic Engng, Vol. 85, 1963, pp.519-527.

(2) Sih, G.C., Engng Fract. Mech., Vol. 5, 1973, pp. 365-377.

(3) Hussain, M.A., Pu, S.L. and Underwood, J., in ASTM STP 560, Amer. Soc.Test. Mat., Phila., USA, 1974, pp. 2-28.

(4) Bhattacharjee, D. and Knott, J.F., Acta metall. et mater., Vol. 42, 1994, pp. 1747-1754.

(5) Bhattacharjee, D. and Knott, J.F., in Mixed Mode Fatigue and Fracture, ESIS 14 (Ed. H.P. Rossmanith and K.J. Miller), M.E.P., London, 1993, pp. 99-109.

(6) Aoki, S., Kishimoto, K., Yoshida, T, Sakata, M. and Richard, H.A., J. Mech. Phys. Solids, Vol. 38, 1990, pp. 195-213

(7) Suresh, S., Shih, C.F., Morrone, A. and O'Dowd, N.P., J. Am. Ceram. Soc., Vol. 73, 1990, pp. 1257-1267.

(8) Knott, J.F., Fundamentals of Fracture Mechanics, Butterworths, 1973.

(9) Bowen, P., PhD thesis, University of Cambridge, 1984.

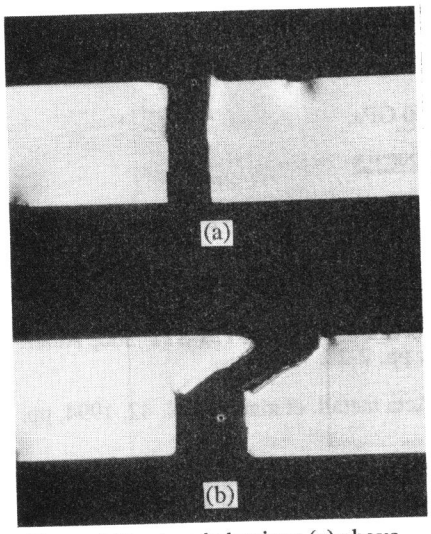

Figure 1 Fracture behaviour (a) above and (b) below transition temperature.

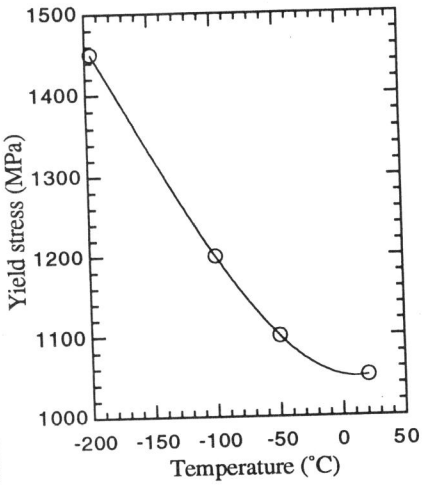

Figure 2 Yield stress (0.2% proof stress) at different temperatures.

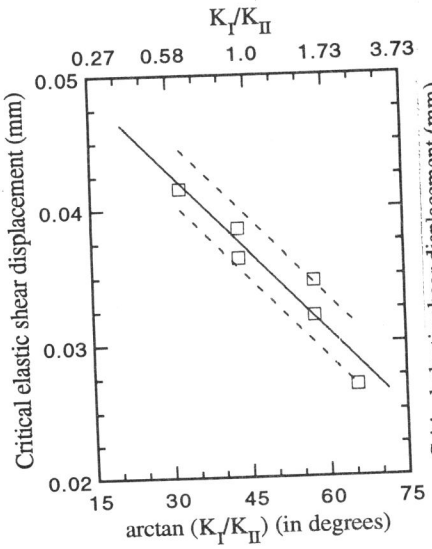

Figure 3 Critical elastic shear displacement corresponding to d_p.

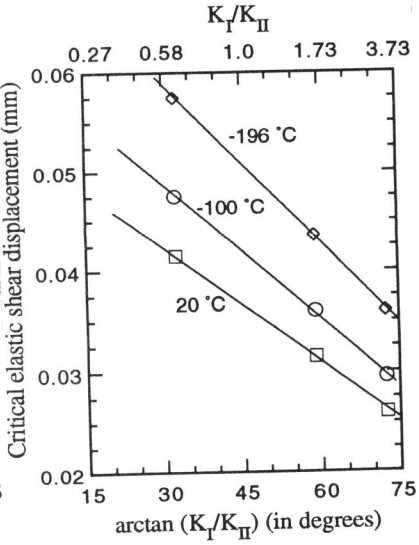

Figure 4 Effect of temperature on the critical elastic shear displacement